*Manuscript
Click here to view linked References

Potential to monitor plant stress using remote sensing tools

[1,3,*]Abel Ramoelo, [2]Sebinasi Dzikiti, [1]Heidi van Deventer, [2]Ashton Maherry, [1]Moses Azong Cho, [2]Mark Gush

[1]Earth Observation Research Group, Natural Resource and Environment, Council for Scientific and Industrial Research, South Africa.
[2]Hydrosciences Research Group, Natural Resource and Environment, Council for Scientific and Industrial Research, South Africa.
[3]University of Limpopo, Risk and Vulnerability Assessment Center, Sovenga, South Africa
*Corresponding author's contact details: Tel: +27(0)12 841 3968, Fax: +27(0)12 841 3968, e-mail: aramoelo@csir.co.za

Abstract

The growing energy crisis has necessitated the expansion of thermal power stations to meet South Africa's electricity needs. Possessing vast amounts of coal deposits, the Waterberg region of the Limpopo Province is set to undergo rapid transformation as new power stations and coal mines are built, expected to exacerbate water shortages. Detailed baseline information to assess future impacts on key plant species is lacking compromising biodiversity conservation efforts in a region where eco – tourism is a major source of livelihood. In this study we evaluated the spatio – temporal distribution plant status during wet and dry seasons using two measures of plant stress namely the midday leaf water potential (LWP), and leaf nitrogen (N) concentrations. At leaf level, spectral indices such as the moisture stress index (MSI), normalized difference water index (NDWI), and the water index (WI) predicted more than 70% of LWP variation using leaf reflectance data. At landscape level, red edge based simple ratio indices were selected for mapping leaf water potential and leaf N for wet and dry season using RapidEye data. We conclude that remote sensing images can be applied for the long term vegetation monitoring for future biodiversity conservation efforts.

Key words: Leaf Nitrogen, Leaf water potential, Hyperspectral, Leaf reflectance, Plant stress, RapidEye imagery, Red Edge band, Vegetation indices.

1. Introduction

Global change including land cover or use and climate changes due to increasing economic activities and growing populations as well as alterations in temperature and precipitation regimes pose major threats to freshwater ecosystems and biodiversity in many catchments (Dye et al., 2008; Everson et al., 2012; Staden and Bredenkamp, 2005; Zhu and Ringler, 2012). These influence water availability to vulnerable ecosystems such as plant communities which are vital sources of food and shelter for animal, bird, and aquatic species. For example, Waterberg region which is relatively pristine in South Africa is set to experience drastic transformation. New thermal power stations and coal mines are being developed to stem a growing energy crisis in South Africa (Corbett et al., 2008; Orbeholster et al., 2010). Waterberg region constitutes close to 50% of the remaining coal reserves in South Africa, and has a huge economic development potential to allay some of the highest unemployment levels (Mgojo, 2012). Besides the coal deposits, the region is also rich in biodiversity inhabiting rare freshwater fish species such as the *Ophrydium versatile,* which are not known to occur anywhere else on the African continent (Orberholster et al., 2010) and rare wetland plant species such as the *Oryza longistaminata* (DWA, 2008), among others.

The planned large scale land use changes in the Waterberg will inevitably have adverse impacts on the environment given that the region is already severely water stressed (Staden and Bredenkamp, 2005). The goal of our study is to provide detailed quantitative information on typical water stress levels of dominant indigenous plant species in the region under the current land and water allocation practices thereby filling an important information gap. We use this information to identify potential remote sensing tools that can be used for future monitoring of plant stress which is expected to worsen as pressure on the limited water resources intensifies. Remote sensing techniques have been used to estimate biophysical parameters (e.g. leaf area index - LAI, biomass) and biochemical parameters (e.g. leaf water content, leaf N and leaf pigments) at scales ranging from local (Dzikiti et al., 2011; Stuckens et al., 2011; Ramoelo et al. 2011) using portable spectrometers to regional scales using air or space-borne sensors (Ramoelo et al. 2011; 2012; 2013). Commonly used approaches employ empirical statistics that

correlate vegetation indices with biophysical or biochemical parameters (Eitel et al., 2008; Ramoelo et al. 2012).

A common challenge in using broad band vegetation indices for plant parameter estimation is the saturation problem (Tucker, 1977). This phenomenon normally occurs during peak vegetative growth phases when the ability of the vegetation indices to detect small changes in plant attributes such as the LAI diminishes (Tucker, 1977; Mutanga and Skidmore, 2004). The saturation problem has been circumvented with the advent of the red edge position (Mutanga and Skidmore, 2004). The red edge position is a second generation of vegetation indices and is known to be positively correlated to pigments and nutrients, mainly chlorophyll and leaf N, minimize background effects (Horler et al., 1983; Cho and Skidmore, 2006). Confirming the importance of the red edge position is the fact that modern satellite sensors are strategically equipped with the red edge band to enable the quantification of biochemical properties of plants such as leaf N concentrations at larger spatial scales (Eitel et al., 2008; Ramoelo et al., 2012). Leaf N concentration is often used as a surrogate measure of vegetation condition or quality (Clifton et al., 1994; Wang et al., 2004). Use of this biochemical property assumes a linear relationship between leaf N and chlorophyll whose concentrations are known to be highly sensitive to plant satus (Yoder and Pettigrew-Crosby, 1995; Hansen and Schjoerring, 2003).

The main objective of the study was to assess the potential of remote sensing tools to monitor plant stress of dominant indigenous woody plant species in the Waterberg region. We used two independent *in situ* measures namely the midday leaf water potential (LWP) (Dzikiti et al., 2013a; Jones, 2004) and the leaf nitrogen concentration (Ramoelo 2011; 2012) as indicators of plant stress.

2. Materials and methods

2.1. Study area

The study was done in riparian and non – riparian areas in the Mokolo River Catchment of the Waterberg District Municipality adjacent to Lephalale town, South Africa (S 23°41'39.24"; E 27°43'46.06", 843 m asl - Fig 1). Most of the water for the proposed developments is expected to

be drawn from the Mokolo dam (S 24°00'53.94", E 27°46'16.35", 915 m asl). Therefore the Mokolo catchment and adjacent areas are expected to experience significant transformation in the coming years. The area has a very dry climate with mean annual rainfall in the range 285 to 560 mm and most of the rain is received during the summer months (October to March). Potential evapotranspiration ranges from 1 800 to 2 000 mm per year (Vermuelen et al., 2011) and maximum temperatures can exceed 40 °C in summer.

The study area had six vegetation types according to the classification by Mucina and Rutherford, (2006). The dominant groups were the Sub tropical alluvial vegetation (AZa 7) found in the south and central parts of the study area (Fig 1). These were dominated by species such as the water berries (*Syzigium spp)* and reeds (*Phragmites spp)* along river courses and *Combretum – Terminalia spp*, *Ziziphus mucronata, and grasses e.g. Panicum spp* further away from the river channel. Table 1 provides further details on the sampled plant species. The northern region of the study area was characterized by low lying or flat areas and the southern region was predominantly hilly with the Mokolo river flowing northwards through the middle of the catchment towards the Limpopo river.

October 2011 was the warmest month (Fig 2a) during the period July 2011 to June 2012 reaching a maximum temperature of 42.7 °C just before the onset of the rainy season. The minimum temperature of about 11.9 °C was recorded in July 2011. Total rainfall was about 338 mm (Fig 2b) during the entire year (July 2011 to June 2012) which was slightly lower than the long term annual average of about 420 mm. As expected, the annual reference evapotranspiration (ET_o) far exceeded rainfall, being 1 611 mm. By the time the summer campaign commenced on 5 December 2011 about 116 mm of rainfall had been received in the Mokolo Catchment with more rainfall (~80 mm) having been received in October. The duration of our summer data collection (5 – 9 December 2011) was dominated by clear skies with no rainfall.

Insert Fig 1, Fig 2, Table 1

2.2. Field data collection

2.2.1. Sampling methods

Data was collected using a purposive and road sampling design because of limited access to the high – fenced game reserves and mine properties that dominate the land use in the study area. We conducted the campaigns during the wet summer season from the 5th to the 9th of December 2011 and again during the dry season from the 18th to the 22nd of June 2012. Sampling of the grasses was done only during the summer season when the grass was green and actively transpiring while trees were sampled during both seasons. However, fewer trees were sampled during the winter season as some species had either shed their leaves or had been cut in some cases. During summer, grass samples were collected in homogenous patches or plots of about 10 – 20 m. In each plot, at least two to three samples were collected from a quadrant sized 50 cm x 50 cm. Five leaves were randomly clipped around the perimeter of the canopy of each sampled tree using a leaf clip to ensure adequate biochemical variability. Samples were collected only from big trees with a canopy diameter of at least six meters to ensure a complete coverage of the RapidEye satellite pixel (~ 5 m x 5 m). For each sampled tree, GPS coordinates were recorded.

2.2.2 Leaf water potential measurements

The grass and tree leaf samples were collected around midday between 1100 and 1500 (Local time = GMT + 2h). The midday LWP was measured within five minutes of the leaves being picked using a Scholander – type pressure chamber (PMS Systems, USA) on between three and five leaves during the summer campaign. A special adapter with a longitudinal slit was used on the head piece of the pressure chamber to measure the water status of natural grass which has rarely been quantified in South Africa as far as we are aware. The measured leaves were immediately cold stored in a cooler box packed with ice blocks to prevent desiccation of the leaves for later measurements of the leaf reflectance.

2.3 Remote sensing data

2.3.1 Hyperspectral remote sensing data

The hyperspectral reflectance spectrum of all the picked leaves was measured using the leaf probe of a portable Analytical Spectral Device (ASD) spectroradiometer (ASD Inc. Boulder, CO, USA) that detects reflectance in the 350 - 2500 nm spectral region. Measurements of the leaf reflectance spectrum were taken as a first step to establish whether the level of water stress on the different vegetation types could be detected using spectral data without background interference as is the case with canopy or catchment level satellite imagery. The spectroradiometer is characterized by a spectral resolution of 3 nm (full-width-at-half-maximum, FWHM) and a 1.4 nm sampling interval across the 350 – 1050 nm spectral range. The FWHM and the sampling interval for the 1051-2500 nm spectral range are 30 nm and 2 nm, respectively. While the measurement of the reflectance spectrum of tree leaves was straightforward, the reflectance of the grass leaves was more difficult given the thin nature of the blades relative to the size of the leaf probe (~ 20 mm diameter). To achieve a full cover of the black spectralon background on the leaf probe we stacked a number of grass blades together forming a thin matt whose thickness was equivalent to that of the individual grass leaves so as not to distort the reflectance in the near infrared wavelengths.

2.3.2 Satellite remote sensing data

The mission to collect the RapidEye satellite images was tasked to coincide with the in situ data collection campaigns in December 2011 and June 2012, respectively. The satellite data was required to predict the status of the indigenous vegetation at the tree and catchment scales. The RapidEye sensor is a multispectral push broom imager with a spatial resolution of 6.25 m and samples light in the spectral bands: blue(440-550 nm), green (520-590 nm), red (630-685 nm), red edge (690-730 nm), and near infrared (760-850 nm) (RapidEye, 2010). The RapidEye Ortho product (Level 3A) was provided with radiometric, sensor, and geometric corrections applied using the digital terrain elevation data (DTED) level 1 Shuttle Radar Terrain Mission (SRTM). The orthorectification accuracy of 1 or less pixel was achieved (RapidEye, 2010). The RapidEye Ortho product was acquired at 5 m x 5 m resampled spatial resolution and this ensured that individual tree canopies could be captured. To retrieve the surface reflectance atmospheric correction was executed using the atmospheric and topographic correction software (ATCOR 2)

implemented in the IDL Virtual Machine (Richter, 2011). ATCOR 2 models reflectance for flat surfaces was selected because the study area was not characterized by very rugged terrain. ATCOR 2 was developed specifically for satellite remote sensing data and includes a large database of atmospheric correction functions (look-up-tables computed with the Modtran® 5 radiative transfer code) which entails a wide range of weather conditions, sun angles, and ground elevations (Richter, 2011). The Modtran® standard aerosols for "rural" were selected to compute the aerosol type, and "visibility" was computed according to Richter (2011). RapidEye metadata were used to obtain additional information for reflectance retrieval such as satellite and solar zenith angle, satellite and solar azimuth angle, as well as relative azimuth angle. The workflow for implementing ATCOR atmospheric correction in any terrain is articulated in Richter (2011).

2.4 Chemical analysis: leaf nitrogen extraction

Finally the leaf samples were taken to the laboratory for leaf N retrieval. The samples were dried at 80 ^{0}C for at least 24 hours and were taken to Bemlab laboratories for chemical analysis. Leaf N values were extracted using a Leco FP528 nitrogen analyser (Horneck & Miller 1998). Climate data was obtained from an automatic weather station located at Werkendam farm situated within the study area.

2.5. Spectral indices

For each GPS tagged sampling point, the reflectance data was carefully extracted from the RapidEye image for analysis. More than 40 commonly used indices for predicting leaf biophysical and biochemical properties were evaluated in this study and these are summarized by Rodriguez – Perez et al (2007). These include some of the most commonly used vegetation indices such as normalized difference vegetation index (NDVI) (Rouse et al. 1976), soil adjusted vegetation index (SAVI) (Huete (1988), MERIS terrestrial chlorophyll index (MTCI) **(**Dash and Curran 2004), simple ratio (SR) (Jordan 1969; Rodriguez – Perez et al. 2007), enhanced vegetation index (EVI) (Huete et al. 2002) as well as the Structure Intensive Pigment (SIPI) (Penuelas et al.1995). The incorporation of the red edge band in computing vegetation indices is known to improve the

prediction of leaf biochemical properties (Ramoelo et al., 2012). Table 2 shows vegetation indices applied on the RapidEye extracted reflectance.

Insert Table 2

2.6. Data analysis

Univariate statistical techniques were used to predict the *in situ* plant stress levels depicted by the LWP and leaf nitrogen concentration (N). To determine which vegetation index highly predicts leaf N or LWP, bootstrapping simple regression was used. Bootstrapping is an unbiased validation technique which iteratively samples data sets from the population with or without replacement (Bunke and Droge, 1984; Efron and Tibshirani, 1997). It samples about two-third of the data sets and predicts a parameter and validates with the remaining one-third iteratively and in this case 1000 times. The bootstrapped Pearson *r* was reported and the corresponding significance level ($p<0.05$). Grass samples were not used when analysing two season RapidEye data for both leaf N and leaf water potential, because the data were collected only in summer.

NDVI thresholding was used to separate trees from non-tree cover (i.e. water, grass, built-up areas and agriculture). The variability of NDVI for different land cover classes was studied and thresholds were selected. It was difficult to remove some of the irrigated agricultural areas, because their NDVI values were similar to those of trees (NDVI>0.4 and 0.5 in dry and wet seasons, respectively). Therefore, a threshold of NDVI<0.4 and <0.5 was used to mask all non-tree features for winter (2012) and summer image (2011) respectively. The method was chosen because it is basic and easy to implement (Cheng et al. 2008).

3. Results

3.1. *In situ* Leaf water potential and leaf N

The leaves were mature and fully expanded on most tree species that we sampled during the summer campaign and Table 3 shows how the midday LWP varied among the species. Generally the grasses tended to have higher levels of water stress than the trees with *Eragrostis rigidior* being the most severely stressed with a mean LWP of – 2.31 MPa. Despite water not

being a limiting factor, the consistently high levels of water stress in *Phragmites* species (< - 1.75 MPa) was not expected. Regarding the trees, the marulas (*Sclerocarya birrea*) had consistently low levels of water stress (> - 0.70 MPa) while the *Combretum – terminalia spp* occurring in non – riparian areas had the highest levels of water stress (< - 1.50 MPa). A mean LWP value as high as -1.31 MPa in summer was also not expected for the water berries (*Syzigium* spp) as the trees were growing along the river channel. The summer data set shows a tendency for the water status of both the trees and grasses to vary between sites although it appeared as if water availability was not always the limiting factor.

Insert Table 3.

There were clear differences in the water status between the winter and summer seasons for most tree species except for the water berries (*Syzigium* spp). Despite the much lower atmospheric evaporative demand in winter, most plants (mainly trees) showed higher levels of water stress with a mean LWP of – 2.31 MPa (for all the tree species) than in summer when the mean LWP was – 1.30 MPa (Table 3). On the other hand, leaf N concentrations varied in the summer and winter seasons with the coefficient of variation (CV) of 33.90 and 20.0%, respectively (Table 4). Leaf N was generally high in the wet than in dry the season, with mean values of 1.78 and 1.47%, respectively (Table 4).

Insert Table 4.

3.2. Correlation of leaf water potential with hyperspectral reflectance data

For leaf level, leaf water potential levels were well predicted by at least six out of the forty spectral indices that we reviewed using the leaf reflectance data (Fig 3). Details of the indices are summarized in Rodriguez – Perez et al (2006) and best performing ones include: 1) the simple ratio 2 (SR2 = R_{1070}/R_{1340}) in Fig 3a; 2, the moisture stress index (MSI = R_{870}/R_{1350}) in Fig 3b; 3) the normalized difference water index (NDWI = $[R_{859}-R_{1240}]/[R_{859}+R_{1240}]$) in Fig 3c; 4) the water band index (WBI = R_{970}/R_{900}) in Fig 3d; 5) the water index (WI = R_{900}/R_{970}) in Fig 3e; and; 6) the enhanced vegetation index (EVI = $[R_{859}-R_{645}]/[R_{859}+6.R_{645}-7.5.R_{469}+1]$) in Fig 3f.

Insert Fig 3.

3.3. Correlation between leaf water potential and satellite remote sensing data

Using spectral indices derived from the RapidEye satellite, the LWP was highly and significantly predicted by the Greenness index (GI), the Red/Green index (RGI), the Green/ Red Ratio (GRR) and the Normalized Green/Red Ratio (NGRR) index which explained over 70% of the variation measured by Pearson *r* during the dry season (June 2012) (Table 5). The Normalized Difference Vegetation Index (NDVI), Simple Ratio (SR), EVI and the Soil Adjusted Vegetation Index (SAVI) explained over 60% of the LWP variation. For the summer data set (December 2011), the MTCI explained over 60% of the LWP variation followed by the RapidEye band (555 nm) predicting about 40% of the variation. For the combined data sets (2011+2012), SR and SIPI1 significantly estimated the LWP explaining about 38% of the variation. The red edge based SR (RE-SR) and EVI were the second best indices for estimating the LWP and performance of the other indices are reported in Table 5. The mathematical formulations of the vegetation indices are given by Rodriguez – Perez et al (2007).

Insert Table 5

3.4. Correlation between leaf nitrogen concentration and satellite remote sensing data

Leaf N concentration was significantly estimated using the Simple Ratio 4 (SR4) and Red Edge based RE_NDVI, explaining 27 and 26% of variation, respectively in 2011 (wet season). For 2012 (dry season) vegetation indices did not significantly explain the variation in leaf N, though the Red Edge Simple Ratio (RE_SR) yielded over 30% of the variation. The combined (2011+2012) data set yielded significantly higher leaf N estimation potential than either the 2011 (wet season) or 2012 (dry season) results alone. The highest prediction was achieved by RE_NDVI and NDVI, explaining over 40% of leaf N variation. SR, RE_SR, 555 nm, 710nm and 805 nm explained over 30% of leaf N variation, and detailed results are presented in Table 6.

Insert Table 6.

3.5. Mapping the spatial variation of plant status using RapidEye

Wet and dry season leaf water potential model based on SR4 (Eq. 1) was used to create leaf water potential maps. Other significant models are based on 555nm, SR, RE_NDVI, SR4 and SIPI1. These models were significant and also have highest Pearson *r*=0.55, RMSE=0.34 MPa.

Leaf water potential (wet/dry) = 2.5476 x SR4 – 2.8027 (1)

For developing leaf N maps, a model based on the RE_SR was used (Eq. 2). A pooled or combined model was selected because of the non-significant model in winter or dry season (2012). Several models were significant and qualified for creating a map, e.g. NDVI, RE_NDVI, 555nm and 710 nm. The equation of the selected model (Pearson *r*=0.36, RMSE = 0.40%) was the following;

Leaf N (%) = 0.16996 x RE_SR + 1.42649 (2)

Plant stress is prevalent in the northern part of the study as depicted by low red edge based simple ratio values in both wet and dry season (Fig. 4). The central and southern part show relatively moderate stress. In essence, about 80 to 90% of the study area does not show water stress in summer. The riparian zones and hilly areas are consistently not stressed in both wet and dry season, as depicted by Figure 5. Figure 6 shows a moderate plant stress in the study area in both dry and wet season, as depicted by leaf water potential. These maps show baseline information about the plant stress in the Waterberg region.

Insert Fig 4, 5 and 6.

4. Discussion

The LWP was successfully estimated and mapped using vegetation indices derived from the RapidEye satellite. Vegetation indices are well known proxies of vegetation greenness (Broge and Leblanc, 2000; Rodriquez – Perez et al., 2007). The vegetation greenness is underpinned by the concentration of pigments, mainly chlorophyll, and water plays an essential part (Eitel et al., 2011). As a result, the correlation between the LWP and the vegetation indices was higher in the dry than in the wet season. The red edge band embedded in the RapidEye spectral data predicted leaf N with higher accuracy in the wet season. Field spectroscopic studies indicated

that the red edge inflexion point, in this context the red edge band, is insensitive to atmospheric and background effects (Ramoelo et al., 2012) and this likely explains why this band was able to predict the leaf N and hence water stress in this study. The results of this study are consistent with other studies that have estimated leaf N at the regional scale (Ramoelo et al. 2012) and using laboratory or field spectroscopy (Mutanga and Skidmore 2007; Gong et al. 2002; Cho and Skidmore 2006; Ramoelo et al., 2013).

Unlike the LWP, estimation of leaf N using vegetation indices was rather difficult during the dry season and we suspect this was because the relationship between leaf N and chlorophyll deteriorated as the leaves senesced (Wenjiang et al. 2004). The univariate models for estimating leaf N were all not significant during the dry season. This shows that phenology plays a crucial role in the estimation of leaf bio-chemical constituents especially associated with leaf greenness and senescence (Knox et al. 2010; Wenjiang et al. 2004). Combining the dry and wet season leaf N data in the model development enabled dry season estimation and mapping of leaf N (Ullah et al. 2012).

For the past three decades hyperspectral remote sensing championed the estimation of leaf biochemical and biophysical parameters at the local scale (Plummer 1988; Mutanga and Skidmore, 2007). A major short coming of this approach has been the failure to estimate biophysical or biochemical parameters at the regional scale to inform decision makers. Nevertheless, the new upcoming satellite sensors with the red edge band such as WorldView 2, RapidEye and SumbandilaSat as well as the upcoming European Space Agency (ESA)'s Sentinel-2 offers opportunities to estimate leaf biochemicals at a regional scale, as demonstrated by this study and Ramoelo et al. (2012) and Cho et al. (2013). These technologies will benefit future biodiversity conservation in the Waterberg and this study provides a useful first step in the early detection of stress in indigenous plants which can be used for designing future early warning systems to inform decision makers on the state of the environment.

Regarding the spatial distribution of plant stress, the northern parts of the study area (Figs 4, 5 & 6), showed the most water stress during both seasons while the central areas had low levels of stress likely because of the prevalence of irrigated agricultural crops. Differences in the dominant

vegetation types between the northern and southern parts of the catchment likely explain the observed variations in the observed stress levels. For example, the northern parts of the catchment in the neighbourhood of Lephalale town has experienced extensive land use changes while riparian areas in the Mokolo river are extensively impacted by rampant sand mining. Grasses and reeds are therefore the dominant vegetation cover in the northern areas and this likely explains the observed higher stress levels. The southern parts of the catchment, on the other hand, were still relatively pristine with a higher density of tree cover in the game farms and nature reserve and these showed less consistent with our *in situ* stress measurements. During the dry season, some of the irrigated agricultural areas were not as visible as the wet season as no winter crops are grown in the area while summer crops are often irrigated due to the infrequent rains. Riparian areas showed minimal changes between the wet and dry periods as water for the plants was always available. Comparison of wet and dry season water stress levels could help to identify naturally induced stresses in order to develop the baseline information that could be used to assess the impact of new land use activities.

This study quantified the water status of dominant tree and, for the first time in the Waterberg, grass species under the current land and water management practices. Grasses appeared to experience more pronounced water stress during the summer season than the adjacent trees. One reason for this could be the fact that trees have access to different sources of water (Dzikiti et al 2013b; Hultine and Bush, 2010) e.g. soil water, groundwater and in some cases river water because of their relatively extensive and deep root system compared to grasses. This observation is supported by results from other studies that have reported higher evapotranspiration rates in tree than grass dominated catchments (Dye et al., 2008; Everson et al., 2011) suggesting that trees likely maintain higher transpiration rates (open stomata) for longer than grasses. Plants rely on the internally stored water to meet the atmospheric evaporative demands during parts of the day (Steppe et al., 2006; Dzikiti et al., 2007). However, high levels of stress can be readily experienced by those species that exhibit anisohydric tendencies when transpiration rates far exceed the rate of water up take leading to the depletion of the internally stored water. The transient imbalance between water uptake by the roots and

transpiration by the canopies can also be a result of a high hydraulic resistance in the transpiration stream (Steppe et al., 2004) although we do not have evidence that this is the case with grasses.

Inefficient hydraulic systems in terms of water transport also quite likely explain the unexpectedly high levels of water stress that we observed on the reeds (*Phragmites spp*) and the *Syzigium spp* given the high atmospheric evaporative demand in the Waterberg. More detailed studies are clearly needed to better understand the water relations and the stress dynamics of the riparian species in the Waterberg. The drought adapted and deep rooted species like the marula (*Sclerocarya birrea*) showed smaller changes in the water status between the wet and the dry seasons compared with other species such as the *Combretum* and *Terminalia spp*. This study also demonstrates that several spectral indices can be used to detect the levels of water stress in indigenous vegetation using leaf reflectance data. While the leaf reflectance information may be used for the rapid assessment of stress levels *in situ*, this leaf level spectral data is unlikely to be useful in the long term monitoring of plant status. Therefore we scaled up our data to the whole plant level using multispectral RapidEye satellite data.

5. Conclusions

Remote sensing techniques can be applied for the long term monitoring of the water status of indigenous vegetation to guide future biodiversity conservation efforts under changing land and water use practices in the Waterberg. Several vegetation indices were found to be significant in predicting the LWP of trees using leaf reflectance data and different sets of spectral indices were obtained that could explain the observed stress levels using canopy level spectral data. This study demonstrated that the LWP and leaf N concentrations are useful measures of stress for the indigenous vegetation in the Waterberg. Significant differences in the water status also occurred between different tree species depending on the hydraulic properties of the plants and also on the site characteristics. Catchment scale maps of the water status of indigenous plants during specific periods were produced based on detailed ground measurements and these maps will be

likely useful references for future assessments of the impacts of the land use changes on the indigenous vegetation in the Waterberg after the planned developments have been implemented.

6. Acknowledgements

We would like to thank Council for Scientific and industrial Research (CSIR)'s Parliamentary Grant (PG) for funding this project. We also like to thank the Farmers' Union in Waterberg for arranging access that enabled field data collection. We thank Corne Engelbrecht for field work, during winter campaign.

7. References

An, H. & Gu, L. 1989. Fast stepwise procedures of selection of variables by using AIC and BIC criteria. Acta Mathematicae Applicatae Sinica (English Series), 5 (1), 60-67.

Bunke, O. & Droge, B. 1984. Bootstrap and cross-validation estimates of the prediction error for linear regression models. The Annals of Statistics, 12 (4), 1400-1424.

Cheng, W., Chang, J., Chang, C., Su, Y., Tu, T. 2008. A fixed-threshold approach to generate high-resolution vegetation maps for IKONOS imagery, Sensors, 8, 4308-4317.

Cho, M. A. & Skidmore, A. K. 2006. A new technique for extracting the red edge position from hyperspectral data: The linear extrapolation method. Remote Sensing of Environment, 101 (2), 181-193.

Cho, M.A., Ramoelo, A., Debba, P., Mutanga, O., Mathieu, R., van Deventer, H., Ndlovu, N. 2013. Assessing the effects of subtropical forest fragmentation on leaf nitrogen distribution using remote sensing data, Landscape Ecology, (Accepted, 5 June 2013)

Clifton, K. E., Bradbury, J. W. & Vehrencamp, S. L. 1994. The fine-scale mapping of grassland protein densities. Grass and Forage Science, 49 (1), 1-8.

Corbett L, West A, Lawson B. 2008. Environmental impact assessment: proposed coal fired power stations and associated infrastructure in the Waterberg. Eskom Holdings Ltd. 1-114.

Darvishzadeh, R., Skidmore, A., Schlerf, M., Atzberger, C., Corsi, & Cho, M.A. 2008. LAI and chlorophyll estimation for a heterogeneous grassland using hyperspectral measurements. ISPRS Journal of Photogrammetry and Remote Sensing, 63 (4), 409-426.

Dawson, T. P. & Curran, P. J. 1998. Technical note a new technique for interpolating the reflectance red edge position. International Journal of Remote Sensing, 19 (11), 2133 - 2139.

DWA, 2008. Intermediate reserve determination study for the surface and groundwater resources in the Mokolo catchment, Limpopo Province. Dept. Water Affairs, South Africa.

Dye, P.J., Jarmain, C., Le Maitre, D.C., Everson, C.S., Gush, M.B., Clulow, A. 2008. Modelling vegetation water use for general application in different categories of vegetation. Water Research Commission of South Africa Report. 1319/1/08.

Dzikiti, S., Schachtschneider, K., Naiken, V., Gush, M., Moses, G., Le Maitre, D.C.. 2013a. Water relations and the effects of clearing invasive *Prosopis* trees on groundwater in an arid environment in the Northern Cape, South Africa. J. Arid. Environ. 90, 103 – 113.

Dzikiti S, Schachtschneider K, Naiken V, Gush M, Le Maitre DC. 2013b. Comparison of water use by alien invasive pine forests growing in riparian and non-riparian zones. Forest Ecology and Management Journal. 293, 92 - 102

Dzikiti S. Verreynne JS, Strever A. 2011. Seasonal variation in canopy reflectance and its application to determine the water status and water use by citrus trees in the Western Cape, South Africa. Agric. For. Meteorol. 151, 1035 –1044.

Dzikiti S, Steppe K, Lemeur R, Milford JR. 2007. Whole-tree level water balance and its implications on stomatal oscillations of young orange trees under natural climatic conditions. Journal of Experimental Botany 58, 1893 - 1901.

Efron, B. & Tibshirani, R. 1997. Improvements on cross-validation: The .632+ Bootstrap Method. Journal of the American Statistical Association, 92 (438), 548-560.

Eitel JUH., Long DS., Gessler PE., Hunt RE. 2008. Combined spectral index to improve ground-based estimates of nitrogen status in dryland wheat. Agronomy Journal. 100, 1694 – 1702.

Eitel, J.U.H., Vierling, L.A., Litvak, M.E., Long, D.S., Schulthess, U., Ager, A.A., Krofcheck, D.J., Stoscheck, L., Broadband, red-edge information from satellites improves early stress detection in a New Mexico conifer woodland, Remote Sensing of Environment, 115 (12), 3640–3646

Everson CS., Dye PJ., Gush MB., Everson TM. 2011. Water use of grasslands, agroforestry systems and indigenous forests. WaterSA. 37, 781 – 788.

Fuentes, D.A., Gamon, J.A.,Qiu, H.L., Sims, D.A., Roberts, D.A. 2011. Mapping Canadian boreal forest vegetation using pigments and water absorption features derived from the AVIRIS sensor, Journal of Geophysical Research, 106, 33565-33577

Gong, P., Pu, R. & Heald, R. C. 2002. Analysis of in situ hyperspectral data for nutrient estimation of giant sequoia. International Journal of Remote Sensing, 23 (9), 1827 - 1850.

Grossman, Y. L., Ustin, S. L., Jacquemoud, S., Sanderson, E. W., Schmuck, G. & Verdebout, J. 1996. Critique of stepwise multiple linear regression for the extraction of leaf biochemistry information from leaf reflectance data. Remote Sensing of Environment, 56 (3), 182-193.

Hansen, P. M. & Schjoerring, J.K. 2003. Reflectance measurement of canopy biomass and nitrogen status in wheat crops using normalized difference vegetation indices and partial least squares regression. Remote Sensing of Environment, 86 (4), 542-553.

Huete, A.R. 1988. A soil-adjusted vegetation index (SAVI). Remote Sensing of Environment, 25, 295-309.

Huete, A. R., Liu, H., Q., Batchily, K. & van Leewen, W. 1997. A comparison of vegetation indices global set of TM images for EOS-MODIS. Remote Sensing of Environment, 59 (3), 440-451.

Horneck, D. A. and Miller, R. O. 1998. Determination of Total Nitrogen in Plant Tissue pp. 75-83. In: Kalra, Y. P. (ed.) Handbook of Reference Methods for Plant Analysis, CRC Press, New York.

Horler, D. N. H., Dockray, M. & Barber, J. 1983. The red edge of plant leaf reflectance. International Journal of Remote Sensing, 4 (2), 273-288.

Huang, Z., Turner, B. J., Dury, S. J., Wallis, I. R. & Foley, W. J. 2004. Estimating foliage nitrogen concentration from HYMAP data using continuum removal analysis. Remote Sensing of Environment, 93 (1-2), 18-29.

Jones, H.G., 2004. Irrigation scheduling: advantages and pitfalls of plant -based methods. J. Exp. Bot. 55, 2427 -2436.

Jordan, C. F. 1969. Derivation of leaf area index from quality of light on the floor. Ecology, 50, 663-666.

Knox, N. M., Skidmore, A. K., Schlerf, M., de Boer, W. F., van Wieren, S. E., van der Waal, C., Prins, H. H. T. & Slotow, R. 2010. Nitrogen prediction in grasses: effect of bandwidth and plant material state on absorption feature selection. International Journal of Remote Sensing, 31 (3), 691-704.

Mgojo, M. 2012. Developing resources in the Waterberg: The Exxaro story. Coaltrans, Southern Africa.

Mucina, L., Rutherford, M.C., 2006. The vegetation of South Africa, Lesotho and Swaziland. Strelitzia 19. South African National Biodiversity Institute, Pretoria.

Mutanga, O. & Skidmore, A. K. 2004. Narrow band vegetation indices overcome the saturation problem in biomass estimation. International Journal of Remote Sensing, 25 (19), 3999 - 4014.

Mutanga, O. & Skidmore, A. K. 2007. Red edge shift and biochemical content in grass canopies. ISPRS Journal of Photogrammetry and Remote Sensing, 62, 34-42.

Orbeholster P, Ashton P, Fritz G, Botha A. 2010. First report on the colony-forming freshwater ciliate Ophrydium *versatile* in an African river. WaterSA 36, 315-322.

Peñuelas, J., Fillela, I., Llolet, P., Munoz, F. & Vilajeliu, M. 1995. Reflectance assessment of mite effects on apple trees. International Journal of Remote Sensing, 16 (14), 2727-2733.

Plummer, S. E. 1988. Exploring the relationships between leaf nitrogen content, biomass and the near-infrared/red reflectance ratio. International Journal of Remote Sensing, 9 (1), 177-183.

Ramoelo, A., Skidmore, A.K., Cho, M.A., Schlerf, M., Mathieu, R., Heitkonig, I.M.A. 2012. Regional estimation of savanna grass nitrogen using the red-edge band of the spaceborne RapidEye sensor. International Journal of Applied Earth Observation and Geoinformation, 19, 151-162

Ramoelo A, Cho MA, Mathieu R, Skidmore AK, Schlerf M, Heitkönig IMA. 2012a. Estimating grass nutrients and biomass as an indicator of rangeland (forage) quality and quantity using remote sensing in Savanna ecosystems. 9th International Conference of the African Association of Remote Sensing and the Environment (AARSE), El Jadida, Morroco, 28 October-2 November 2012, pp 8pp.

Ramoelo, A., Skimore, A.K., Mathieu, R., Heitkönig, I.M.A., Dudeni-Tlhone, N., Schlerf, M., Prins, H.H.T. 2013. Non-linear partial least square regression increases the estimation accuracy of grass nitrogen and phosphorus using in situ hyperspectral and environmental data, ISPRS Journal of Photogrammetry and Remote Sensing, 82, 27-40

Ramoelo, A., Skidmore, A.K., Schlerf, M., Mathieu, R. & Heitkönig, I.M.A. 2011. Water-removed spectra increase the retrieval accuracy when estimating savanna grass nitrogen and phosphorus concentrations. ISPRS Journal of Photogrammetry and Remote Sensing, 66 (4), 408-417.

Rapideye 2010. RapidEye Standard Image Product Specification, Version 3.0, Germany, www.rapideye.de accessed on April 2010.

Richter, R. 2011. Atmospheric/Topographic fro Satellite Imagery (ATCOR 2/3 User Guide, Version 8), Wessling, Germany, DLR-German Aerospace Center.

Rodriguez-Perez, J.R., Riano, D., Carlisle, E., Ustin, S., Smart, D.R. 2007.Evaluation of hyperspectral reflectance indices to detect grapevine water status in vineyard, American Journal of Enology and Viticulture, 58(3), 302-317

Rouse, J. W., Haas, R. H., Schell, J. A., Deering, D. W. & Harlan, J. C. 1974. Monitoring the vernal advancement and retrogradation of natural vegetation. NASA/GSFC, Type III Final Report. M.D. Greenbelt, 371.

Sakamoto, Y., Ishiguro, M. & Kitagawa, G. 1986. Akaike Information Criteria Statistics, US, D. Reidel Publishing Company.

Schleicher, T. D., Bausch, W. C., Delgado, J. A. & Ayers, P. D. 2001. Evaluation and refinement of the nitrogen reflectance index (NRI) for site-specific fertilizer management. Paper number 011151, ASAE Annual Meeting, St. Joseph, Michigan.

Smith, R. C. G., Adams, J., Stephens, D. J. & Hick, P. T. 1995. Forecasting wheat yield in a Mediterranean type of environment from the NOAA satellite. Australian Journal of Agricultural Research, 46 (1), 113-125.

Staden P, Bredenkamp G. 2005. Major plant communities of the Marakele National Park. Koedoe 48, 59-70.

Steppe K. 2004. Diurnal dynamics of water flow through trees: design and validation of a mathematical flow and storage model. PhD thesis, Ghent University, Belgium.

Steppe K, De Pauw DJW, Lemeur R, Vanrolleghem PA. 2006. A mathematical model linking tree sap flow dynamics to daily stem diameter fluctuations and radial stem growth. *Tree Physiology* 26, 257 – 273.

Stuckens J, Dzikiti S, Verreynne JS, Verstraeten WW., Swennen R, Coppin P. 2011. Physiological interpretation of a hyperspectral time series in orchards. Agricultural and Forest Meteorology. 151, 1002 – 1015.

Tucker, C. J. 1977. Asymptotic nature of grass canopy spectral reflectance. Applied Optics, 16 (57-1151).

Vermuelen PD., Bester M., Cruywagen LM., van Tonder GJ. 2011. Scoping level assessment of how water quality and quantity will be affected by mining method and mining of the shallow Waterberg coal reserves west of the Daarby fault. Water Research Commission Report, Pretoria - WRC Report No. 1830/1/10.

Wang, Z. J., Wang, J. H., Liu, L. Y., Huang, W. J., Zhao, C. J. & Wang, C. Z. 2004. The prediction of grain protein in winter wheat (*Triticum aestivum*) using plant pigment ratio (PPR). Field Crops Research, 90, 311-321.

Wenjiang, H., Jihua, W., Zhijie, W., Jiang, Z., Liangyun, L. & Jindi, W. 2004. Inversion of foliar biochemical parameters at various physiological stages and grain quality indicators of winter wheat with canopy reflectance. International Journal of Remote Sensing, 25 (12), 2409-2419.

Yoder, B. J. & Pettigrew-Crosby, R. E. 1995. Predicting nitrogen and chlorophyll content and concentrations from reflectance spectra (400-2500 nm) at leaf and canopy scales. Remote Sensing of Environment, 53 (3), 199-211.

Zarco-Tejada, P.J., Berjon, A., Lopex-Lozano, R, Miller, J.R., Martin, P., Cachorro, V., Gonzalez, M.R. and de Frutos, A. 2005. Assessing vineyard condition with hyperspectral indices: Leaf and canopy reflectance simulation in a row-strucured discontinuous canopy. Remote Sensing of Environment, 99, 271-287

Zhu T, Ringler C. 2012. Climate change impacts on water availability and use in the Limpopo river basin. Water 4, 63-84

***Highlights (for review)**

Highlights

- Leaf water potential and leaf nitrogen used as an indicator of plant stress
- Vegetation indices with red-edge band provide opportunity to monitor plant stress
- Leaf water potential mapped for the first time at landscape level
- Remote sensing has potential for environmental monitoring

Figure1
Click here to download high resolution image

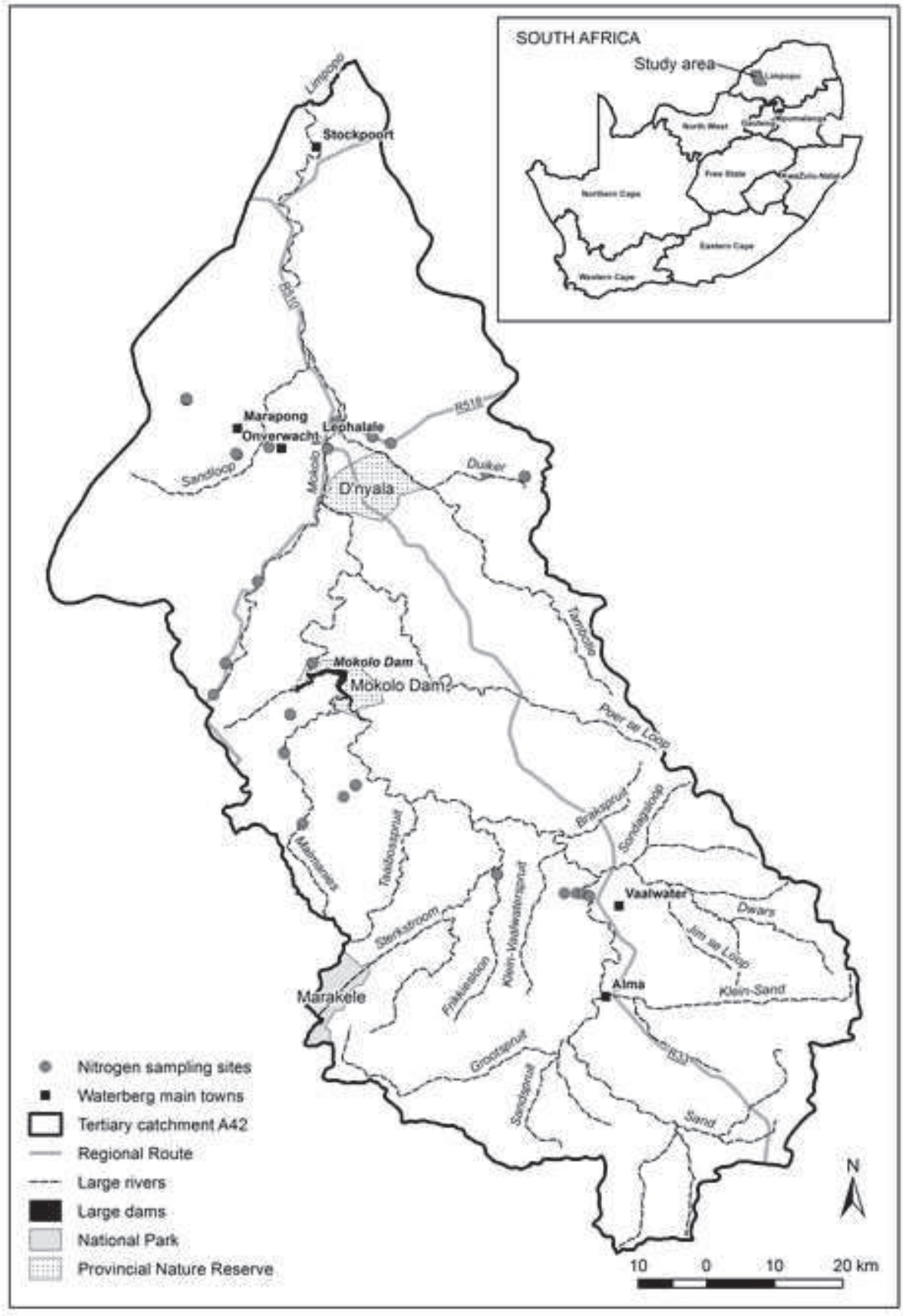

Figure 2

Click here to download high resolution image

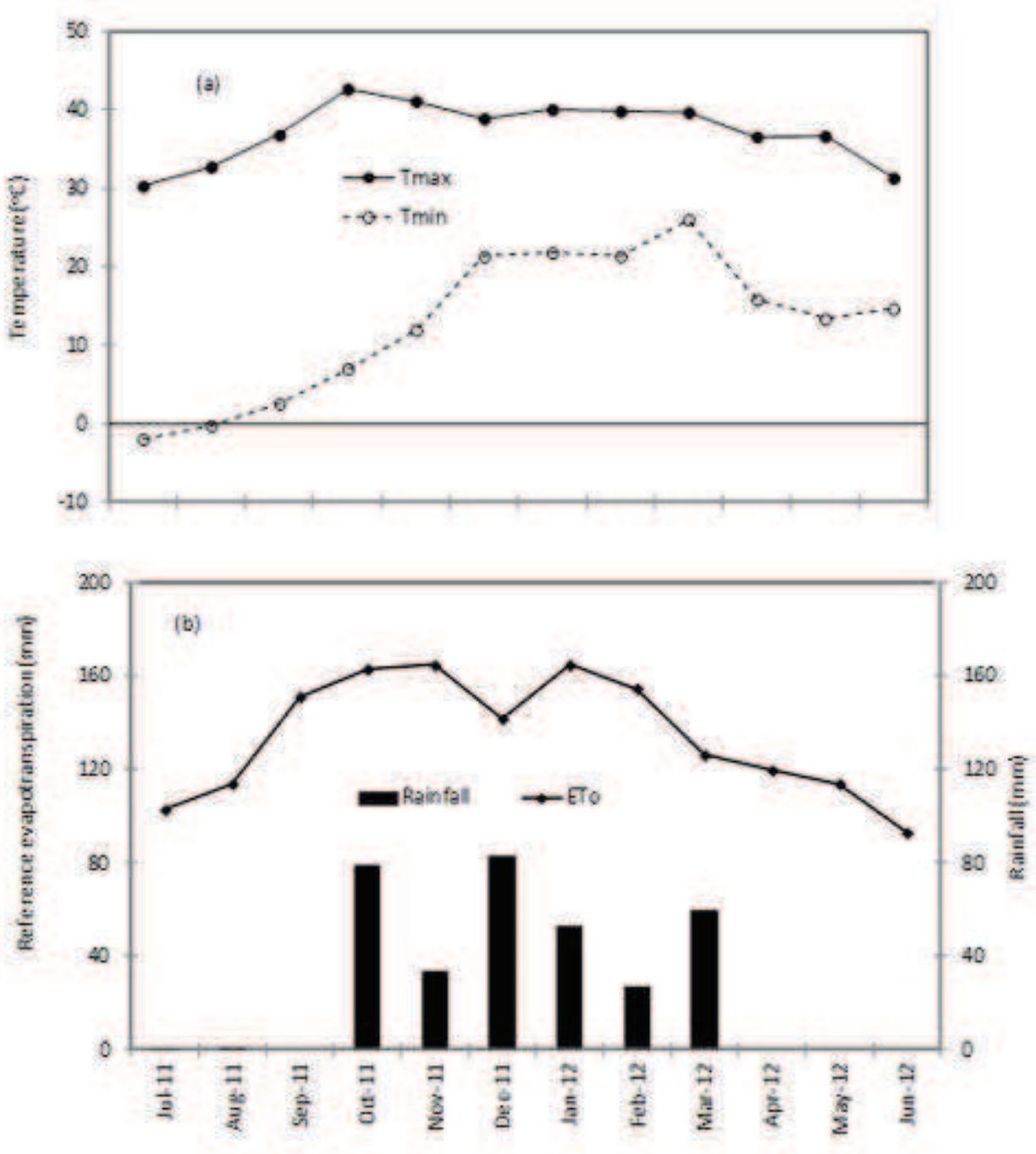

Figure 3
Click here to download high resolution image

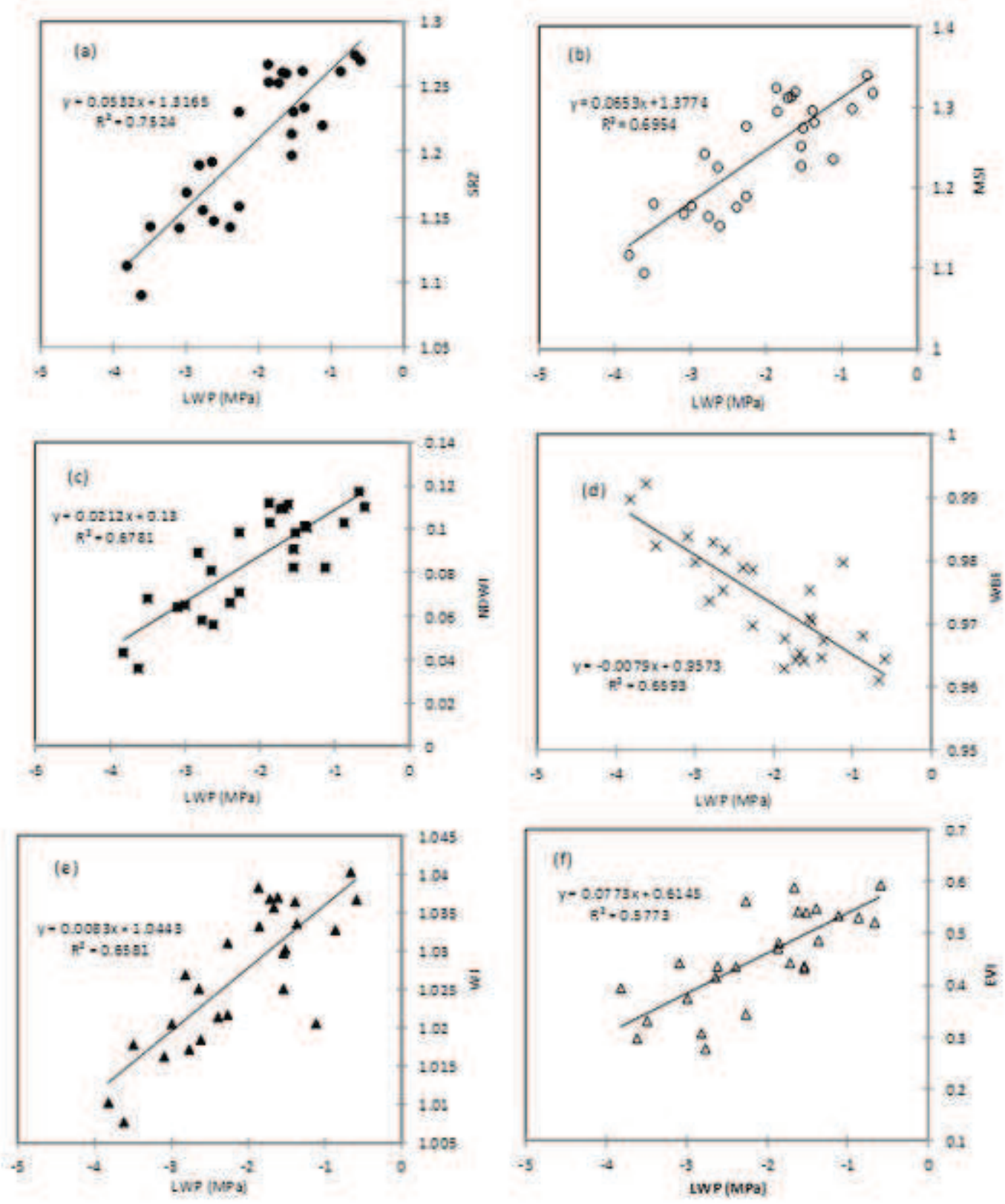

Figure 4

Click here to download high resolution image

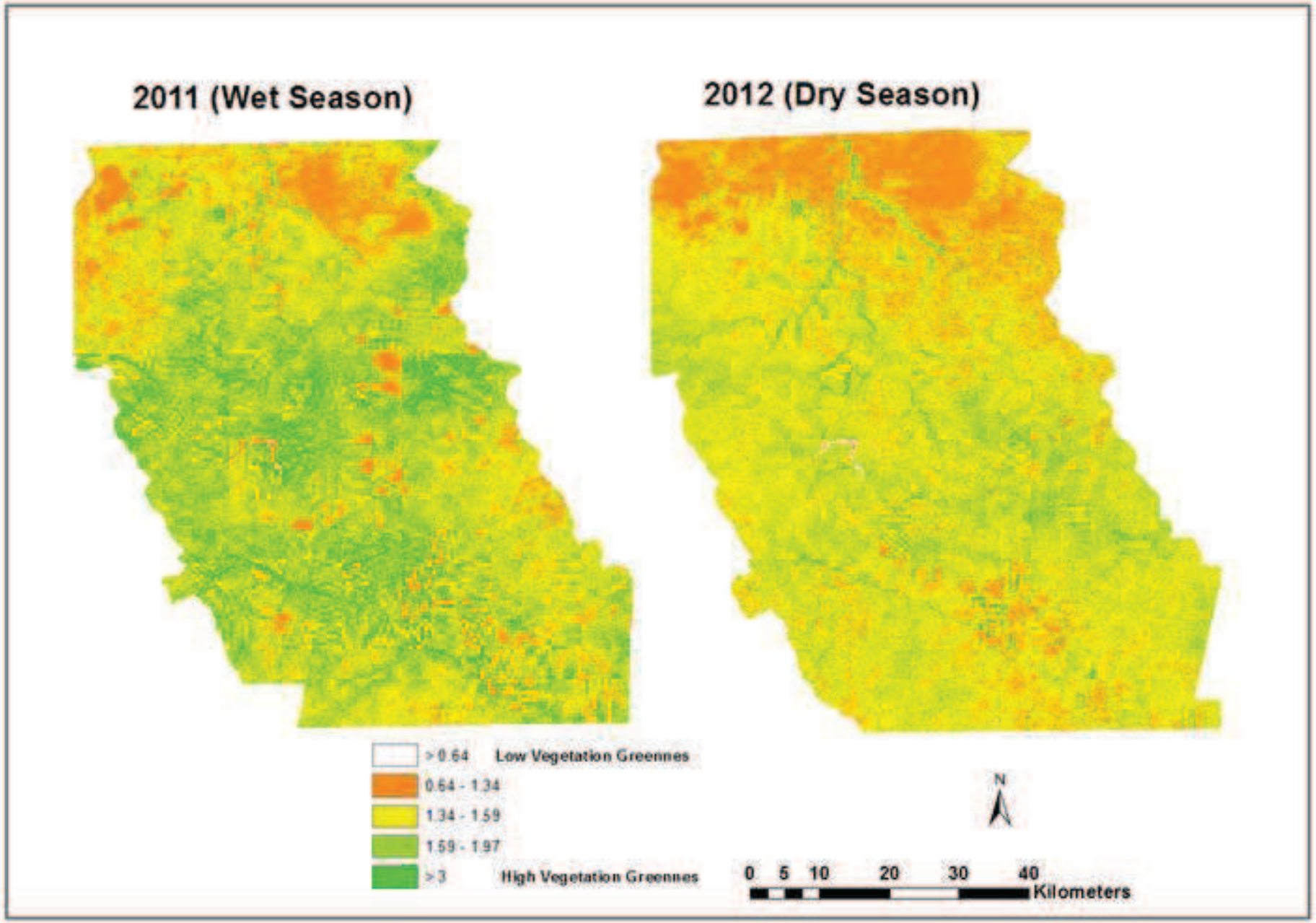

Figure 5

Click here to download high resolution image

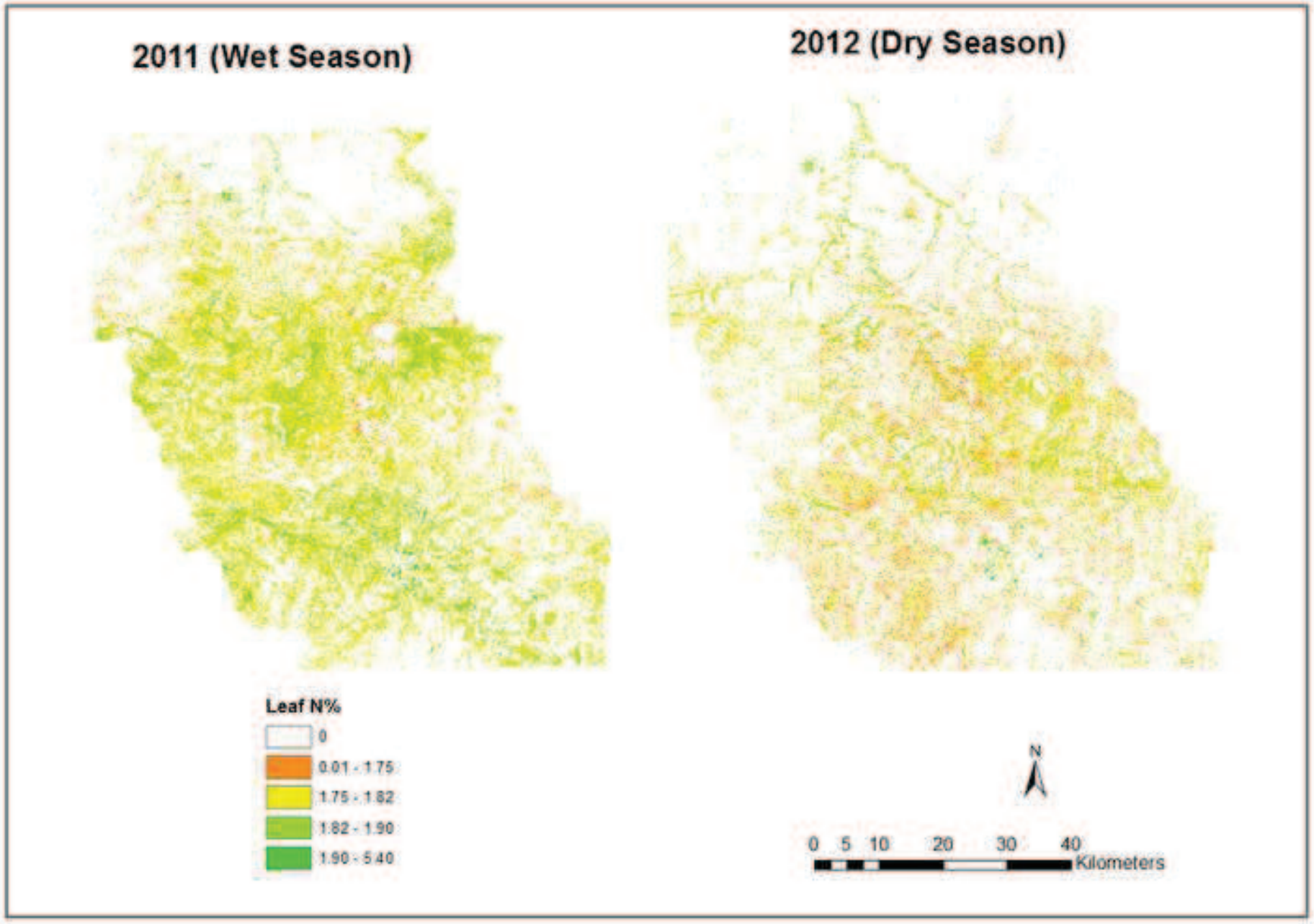

Figure 6

Click here to download high resolution image

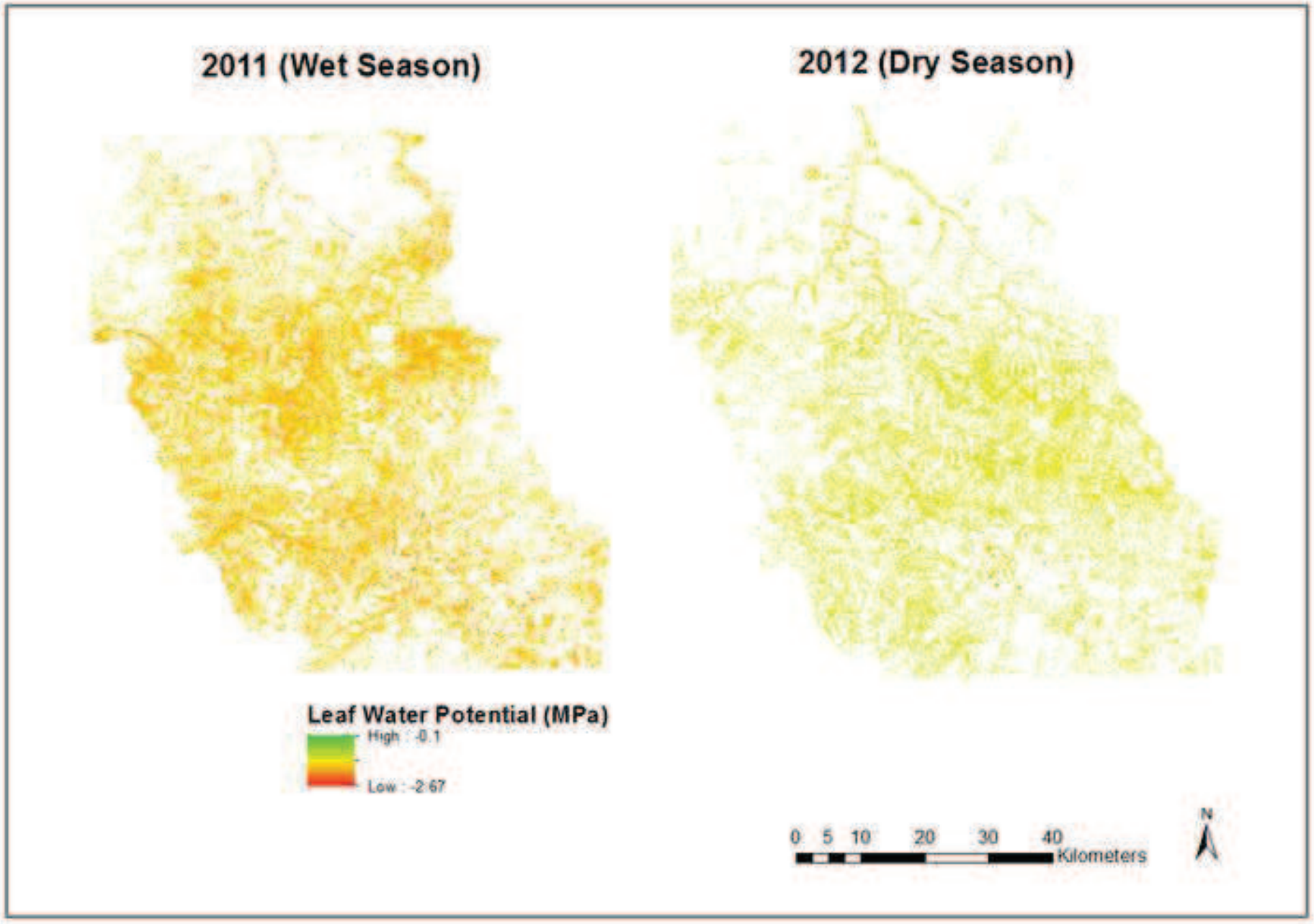

Tables

Table 1: Plant species whose stress levels were determined during both the summer and winter periods. Grasses were sampled only during the rainy season as they had senesced during the dry season (2012).

Scientific name	Common name	Biome
Combretum zeyheri	Large fruited bush willow	SVcb 19/ SVcb 17
Sclerocalya birrea	Marula	Aza 7/ SVcb 12/ SVcb 19
[1]*Panicum maximum*	Buffalo grass	Aza 7/ SVcb 12
[1]*Setaria sphaselata*	African bristle grass	SVcb 19
Combretum imberbe	Leadwood	Aza 7
[1]*Eragrostis rigidior*	Curly leaved love grass	Aza 7
[1]*Panicum coloratum*	White buffalo grass	Aza 7
[1]*Aristida spp*	-	Aza 7
Ziziphus mucronata	Buffalo thorn	Aza 7
Combretum terminalia	-	SVcb 17
[1]*Phragmites Australis*	Common reed	Aza 7
Lannea discolour	Dikbas	SVcb 16/ SVcb 17
Heteropogon contorntus	Tussock grass	SVcb 19
Superba contorntus	-	-
Syzigium cordatum	Water berry	Aza 7
Lannea. Stuhlmannii	False marula	SVcb 16

[1] denotes grasses.

12 Table 2: broadband based vegetation indices used in this study

Indices	Equation	Reference
Normalized Difference Vegetation index (NDVI)	$(R_{805}-R_{657.5})/(R_{805}+R_{657.5})$	Rouse et al., (1974)
Red edge based NDVI	$(R_{805}-R_{710})/(R_{805}+R_{710})$	Ramoelo et al., (2012)
Simple Ratio (SR)	$R_{805}/R_{657.5}$	Jordan, 1969
Red edge based SR (RE_SR)	R_{805}/R_{710}	Ramoelo et al., (2012)
SR3	$R_{657.5}/R_{805}$	Rodriguez-Perez, et al., (2007)
SR4	R_{710}/R_{805}	Rodriguez-Perez, et al., (2007)
MERIS Terrestrial Chlorophyll Index (MERIS)	$(R_{805}-R_{710})/(R_{710}-R_{657.5})$	Dash and Curran, (2004)
Greenness Index (GI)	$R_{555}/R_{657.5}$	Smith et al., (1995)
Red/Green index (RGI)	$R_{657.5}/R_{555}$	Feutes et al., (2001)
RGI1	R_{710}/R_{555}	Zarco-Tejada et al., (2005)
Blue/Green Index (BGI)	R_{475}/R_{555}	Zarco-Tejada et al., (2005)
Blue/Red Index (BRI)	R_{475}/R_{710}	Zarco-Tejada et al., (2005)
Green/Red Ration (GRR)	$R_{555}/R_{657.5}$	Feutes et al., (2001)
Normalized Green/Red Ratio (NGRR)	$(R_{657.5}-R_{555})/(R_{657.5}+R_{555})$	Rodriguez-Perez, et al., (2007)
NGRR1	$(R_{710}-R_{555})/(R_{710}+R_{555})$	Rodriguez-Perez, et al., (2007)
Difference Vegetation Index (DVI)	$R_{805}-R_{710}$	Jordan, 1969
DVI1	$R_{805}-R_{657.5}$	
Simple Ratio Pigment Index (SRPI)	R_{475}/R_{710}	Penuelas et al., (1995)
Structure Insensitive Pigment Index (SIPI)	$(R_{805}-R_{475})/(R_{805}-R_{657.5})$	Penuelas et al., (1995)
SIPI1	$(R_{710}-R_{475})/(R_{710}-R_{657.5})$	
Enhanced Vegetation Index (EVI)	$2.5*(R_{805}-R_{657.5})/R_{805}+(6*R_{657.5})-(7.5*R_{475})+1$	Huete et al., (1997)
Nitrogen Reflectance Index (NRI)	$(R_{555}-R_{657.5})/(R_{555}+_{657.5})$	Schleicher et al., (2001)
Soil-Adjusted Vegetation Index (SAVI)	$((1+0.2)*R_{805}-R_{710})/((R_{805}+R_{710})+0.2)$	Huete, 1988)
SAVI1	$((1+0.2)*R_{805}-R_{657.5})/((R_{805}+R_{657.5})+0.2)$	

13

14

15

16

17

18

Table 3: Midday leaf water potential for plant species in the Mokolo catchment on typical clear days during wet (summer) and dry (winter) seasons.

Species	$\Psi_{L\,max}$ (MPa)	$\Psi_{L\,min}$ (MPa)	$\Psi_{L\,ave}$ (MPa)	Biome
Terminalia-combretum (n=15)	-1.35	-1.80	-1.56	SVcb 12
Sclerocarya birrea (n = 15)	-0.35	-0.65	-0.52	Aza 7
[1]*Panicum maximum (n = 3)*	-2.25	-4.00	-3.03	Aza 7
Combretum zeyheri (n = 10)	-0.65	-2.80	-1.35	SVcb 19
Sclerocarya birrea (n = 5)	-0.75	-0.95	-0.84	SVcb 12
[1]*Panicum maximum (n = 11)*	-0.80	-1.25	-1.11	SVcb 12
[1]*Setaria sphacelata (n = 3)*	-1.26	-1.78	-1.53	SVcb 19
[1]*Heteropogon contorntus (n=3)*	-1.65	-2.25	-1.85	SVcb 19
Sclerocarya birrea (n = 10)	-0.50	-0.90	-0.68	SVcb 19
[1]*Eragrostis rigidior (n = 3)*	-3.35	-3.70	-3.58	Aza 7
[1]*Panicum coloratum (n = 3)*	-2.00	-2.45	-2.16	Aza 7
[1]*Aristida spp (n = 3)*	-2.25	-3.00	-2.54	Aza 7
Combretum imberbe (n = 15)	-1.14	-1.72	-1.35	Aza 7
Sclerocarya birrea (n = 5)	-0.30	-0.65	-0.46	Aza 7
Ziziphus mucronata (n = 5)	-1.45	-2.10	-1.73	SVcb 17
[1]*Phragmitise Australis (n = 4)*	-1.75	-3.36	-2.60	Aza 7
Lannea stuhlmanni (n = 5	-1.20	-1.48	-1.37	SVcb 16
Syzigium cordatum (n = 15)	-0.85	-2.00	-1.33	Aza 7
Combretum zeyheri (n = 6)	-2.25	-3.70	-2.88	SVcb 19
Sclerocarya birrea (n = 6)	-1.45	-3.90	-2.76	SVcb 19
Combretum imberbe (n = 6)	-1.73	-3.15	-2.43	Aza 7
VGT (Unknown)	-1.15	-3.55	-2.09	Aza 7
Syzigium cordatum (n = 15)	-0.60	-2.10	-1.43	Aza 7
[1]*Phragmitise Australis (n=15)*	-3.20	-3.65	-3.48	Aza 7
Sclerocarya birrea (n = 6)	-0.75	-3.20	-1.70	SVcb 16
Lannea discolor (n = 6)	-1.45	-1.65	-1.55	SVcb 16
Lannea discolor (n=6)	-1.25	-3.30	-2.51	SVcb 17

[1] Denotes grasses and the numbers in brackets in column 1 depict the number of leaves.

Table 4: Summary of the descriptive statistics for leaf water potential (trees only) and leaf nitrogen concentrations (trees + grasses)

Variables	Data	Min	Max	mean	SD	CV
Leaf Water Potential (MPa)	2011	-2.60	-0.46	-1.31	0.62	-
	2012	-3.48	-1.43	-2.31	0.68	-
	2011+2012	-3.48	-0.46	-1.74	0.81	-
Leaf Nitrogen (%)	2011	0.93	4.18	1.78	0.60	33.90
	2012	0.93	2.08	1.47	0.29	20.00
	2011+2012	0.93	4.18	1.66	0.53	32.00

CV=coefficient of variance, SD=standard deviation

Table 5: Simple correlation between the midday leaf water potential and various vegetation indices derived from the RapidEye spectral data.

Data	2011 (Wet Season)		2012 (Dry Season)		Combined (2011+2012)	
Bands/Indices	**Pearson *r***	***P***	**Pearson *r***	***P***	**Pearson *r***	***P***
R475 nm	0.34	0.1424	0.15	0.5936	**0.33**	**0.0529**
R555 nm	**0.44**	**0.0522**	0.06	0.8318	**0.37**	**0.0287**
R657.50 nm	0.17	0.4737	0.45	0.0924	0.32	0.0609
R710 nm	0.36	0.1190	0.03	0.9155	0.25	0.1475
R805 nm	0.09	0.7059	-0.43	0.1096	-0.10	0.5676
NDVI	-0.16	0.5004	**-0.61**	**0.0157**	-0.32	0.0609
RE_NDVI	-0.37	0.1083	**-0.53**	**0.0421**	**-0.36**	**0.0337**
SR	-0.19	0.4224	**-0.64**	**0.0102**	**-0.38**	**0.0243**
RE_SR	-0.38	0.0984	**-0.55**	**0.0337**	**-0.37**	**0.0287**
MTCI	**-0.61**	**0.0043**	-0.11	0.6963	-0.29	0.0910
GI	0.38	0.0984	**-0.79**	**0.0005**	-0.01	0.9545
RGI	-0.38	0.0984	**0.78**	**0.0006**	0.05	0.7755
RGI1	-0.29	0.2149	-0.01	0.9718	-0.26	0.1315
BGI	-0.05	0.8342	0.16	0.5689	0.04	0.8195
BRI	0.28	0.2318	-0.44	0.1007	-0.01	0.9545
GRR	0.38	0.0984	**-0.79**	**0.0005**	-0.01	0.9545
NGRR	-0.38	0.0984	**0.79**	**0.0005**	0.03	0.8642
NGRR1	-0.42	0.0652	0.35	0.2009	-0.32	0.0609
SR3	0.15	0.5279	**0.59**	**0.0206**	0.30	0.0800
SR4	0.36	0.1190	**0.52**	**0.0469**	**0.55**	**0.0393**
DVI	-0.07	0.7693	**-0.57**	**0.0265**	-0.26	0.1315
DVI1	-0.28	0.2318	**-0.57**	**0.0265**	-0.31	0.0699
SRPI	0.28	0.2318	-0.44	0.1007	-0.01	0.9545
SIPI	-0.24	0.3081	**-0.54**	**0.0377**	**-0.36**	**0.0337**
SIPI1	-0.35	0.1303	-0.49	0.0637	**-0.38**	**0.0243**
EVI	-0.22	0.3513	**-0.60**	**0.0181**	**-0.37**	**0.0287**
SAVI	-0.16	0.5004	**-0.61**	**0.0157**	-0.32	0.0609
SAVI1	-0.37	0.1083	**-0.53**	**0.0421**	**-0.36**	**0.0337**

Values highlighted in **BOLD** depict significant correlations (p<0.05)

41 Table 6: Simple correlation between Leaf Nitrogen and the RapidEye vegetation indices.

Leaf N (%)	**2011 (Wet Season)**		**2012 (Dry Season)**		**Combined (2011+2012)**	
Bands/Indices	**Pearson *r***	***p***	**Pearson *r***	***p***	**Pearson *r***	***P***
R475 nm	0.13	0.3351	0.12	0.4990	**0.32**	**0.0020**
R555 nm	0.20	0.1357	0.22	0.2112	**0.38**	**0.0002**
R657.50 nm	0.09	0.5055	0.17	0.3364	**0.24**	**0.0210**
R710 nm	0.29	0.0286	0.18	0.3083	**0.33**	**0.0014**
R805 nm	0.13	0.3351	-0.04	0.8223	**0.32**	**0.0020**
NDVI	-0.04	0.7676	-0.21	0.2332	**-0.45**	**0.0000**
RE_NDVI	**-0.26**	**0.0507**	-0.30	0.0847	**-0.48**	**0.0000**
SR	-0.06	0.6575	-0.24	0.1715	**0.34**	**0.0010**
RE_SR	-0.25	0.0607	-0.31	0.0743	**0.36**	**0.0005**
MTCI	-0.38	0.0266	-0.21	0.2332	0.02	0.8507
GI	0.09	0.5055	0.01	0.9552	**0.23**	**0.0283**
RGI	-0.12	0.3739	-0.01	0.9552	**-0.23**	**0.0283**
RGI1	0.12	0.3739	-0.16	0.3660	**-0.24**	**0.0219**
BGI	-0.04	0.7676	-0.10	0.5736	-0.05	0.6378
BRI	-0.10	0.4592	-0.01	0.9552	0.13	0.2193
GRR	0.09	0.5055	0.01	0.9552	**0.23**	**0.0283**
NGRR	-0.11	0.4153	-0.01	0.9552	**-0.23**	**0.0283**
NGRR1	-0.06	0.6575	0.07	0.6940	0.17	0.1071
SR3	0.02	0.8826	0.20	0.2567	-0.07	0.1071
SR4	**0.27**	**0.0422**	0.29	0.0961	-0.01	0.9250
DVI	-0.15	0.2654	-0.18	0.3083	0.20	0.0573
DVI1	0.08	0.5541	-0.12	0.4990	**0.26**	**0.0128**
SRPI	-0.10	0.4592	-0.01	0.9552	0.13	0.2193
SIPI	-0.05	0.7118	0.15	0.3971	-0.15	0.1558
SIPI1	-0.21	0.1169	0.07	0.6940	-0.07	0.5096
EVI	-0.02	0.8826	0.14	0.4297	-0.06	0.5721
NRI	0.11	0.4153	0.01	0.9552	**0.23**	**0.0283**
SAVI	-0.26	0.0507	-0.30	0.0847	0.00	1.0000
SAVI1	-0.04	0.7676	-0.21	0.2332	0.05	0.6379

42 Values highlighted in **BOLD** depict significant correlations ($p<0.05$)

Figure captions

Figure 1: Map of the study area and the location of sampling sites at the Waterberg region, Limpopo

Figure 2: Climatic variables during the study period from July 2011 to June 2012 with (a) showing the trend in the maximum (Tmax) and minimum (Tmin) temperatures and (b) shows the evolution of the reference evapotranspiration (ETo) and the rainfall, respectively.

Figure 3: The relationship between leaf water potential and several vegetation indices (MSI=Moisture Stress Index, EVI=Enhanced Vegetation Index, NDWI=Normalized Difference Water Index, WI=Water Index, WBI=Water Band Index)

Figure 4: Spatial distribution of plant greenness based on red edge-based simple ratio vegetation index during the wet and dry season in the Waterberg (December 2011 and June 2012).

Figure 5: Spatial distribution of leaf nitrogen as an indicator of plant stress during the wet and dry seasons in the Waterberg.

Figure 6: Spatial distribution of leaf water potential as an indicator of plant stress during the wet and dry seasons in the Waterberg.

KML File (for GoogleMaps)

Click here to download KML File (for GoogleMaps): Study Area_Waterberg Regionn_Tertiary catchment A42.kml